TISSUE ENGINEERING: Part A
Volume 16, Number 9, 2010

DOI: 10.1089/ten.tea.2009.0695

The Design of *In Vitro* Liver Sinusoid Mimics Using Chitosan–Hyaluronic Acid Polyelectrolyte Multilayers

Yeonhee Kim, M.S., Adam L. Larkin, B.S., Richey M. Davis, Ph.D., and Padmavathy Rajagopalan, Ph.D.

Interactions between hepatocytes and liver sinusoidal endothelial cells (LSECs) are essential for the development and maintenance of hepatic phenotypic functions. We report the assembly of three-dimensional liver sinusoidal mimics comprised of primary rat hepatocytes, LSECs, and an intermediate chitosan–hyaluronic acid polyelectrolyte multilayer (PEM). The height of the PEMs ranged from 30 to 55 nm and exhibited a shear modulus of ~100 kPa. Hepatocyte–PEM cellular constructs exhibited stable urea and albumin production over a 7-day period, and these values were either higher or similar to cells cultured in a collagen sandwich. This is of significance because the thickness of a collagen gel is ~1000-fold higher than the height of the chitosan–hyaluronic acid PEM. In the hepatocyte–PEM–LSEC liver-mimetic cellular constructs, LSEC phenotype was maintained, and these cultures exhibited stable urea and albumin production. CYP1A1/2 activity measured over a 7-day period was significantly higher in the hepatocyte–PEM–LSEC constructs than in collagen sandwich cultures. A 16-fold increase in CYP1A1/2 activity was observed for hepatocyte–PEM–10,000 LSEC samples, thereby suggesting that interactions between hepatocytes and LSECs are critical in enhancing the detoxification capability in hepatic cultures *in vitro*.

Introduction

The liver is one of the largest organs in our bodies and performs a multitude of functions such as metabolism and detoxification, and plays a major role in the body's complex defense mechanisms. The deterioration in any one of the liver's functions can cause serious, life-threatening health problems. The liver is comprised of ~70% hepatocytes (parenchymal cells) and the remainder is made up of nonparenchymal (liver sinusoidal endothelial, Kupffer, and hepatic stellate) cells.[1] Liver sinusoids *in vivo* contain layers of hepatocytes and endothelial cells separated by the Space of Disse comprised primarily of collagen fibers.[1]

The lack of organ donors, the rising cost of organ transplant surgeries, and the complications related to immune response are issues that confront patients. The use of extracorporeal liver-assist devices, also known as bio-artificial livers, have the potential to enable the recovery of patients with injured livers or function as a bridge to transplantation.[2]

The design of extracorporeal liver-assist devices can be accelerated if three-dimensional (3D) liver mimics are available to systematically test cellular response to a variety of stimuli. In addition, the testing of drugs and pharmaceuticals is conducted on monolayers of hepatocytes or on animals. Hepatocyte monolayers do not present a physiologically relevant model, and animal models can be very expensive and complex to analyze. Although two-dimensional cell cultures and cocultures are used extensively as model systems,[3–10] they do not recapitulate key spatial, geometric, and physiological characteristics of cellular architectures found *in vivo*. The complex heterotypic interactions between parenchymal (hepatocytes) and nonparenchymal (liver sinusoidal endothelial cell [LSEC]) cells in the liver are responsible for optimal hepatic function. Recent reports in the literature have shown that even at the embryonic stage, interactions between endothelial cells and hepatic progenitor cells are critical for normal liver development.[11–13] Since interactions between the parenchymal and nonparenchymal cells of the liver are critical in maintaining optimal hepatic function,[14–16] efforts to layer these cells to emulate liver architecture *in vivo* are ongoing. Recently, new approaches to form layered 3D liver-like tissues have been reported.[17–22] Temperature-responsive culture dishes, magnetic liposome technology, and organ-printing techniques have been utilized to form layered cell sheets. A temperature responsive polymer (*N*-isopropyl acrylamide) was used to release aortic endothelial cells as a sheet and then placed above a monolayer of hepatocytes to form a sinusoidal structure.[17] In other reports, magnetic cationic liposomes were introduced into endothelial cells, which were subsequently placed above hepatocytes to form a layered hepatic construct.[20] Although these methodologies offer new avenues to assemble liver mimics, issues related to long-term stability and ease in handling and assembly are of concern.

Department of Chemical Engineering, Virginia Polytechnic Institute and State University, Blacksburg, Virginia.

The distance of separation between hepatocytes and endothelial cells in the liver, the Space of Disse, is a critical factor in assembling liver-mimetic tissues.[23] *In vitro*, the presence of an interfacial region has been shown to play a significant role in the assembly and performance of liver mimics. In a previous report, hepatocytes and human umbilical vein endothelial cells (HUVECs) were assembled in stratified layers by incorporating a chitosan–DNA polyelectrolyte multilayer (PEM) between the cell layers.[23] This study demonstrated the need for an interface between hepatocytes and HUVECs to obtain optimal hepatic phenotypic function and showed that PEMs could potentially mimic and function as the Space of Disse *in vitro*. Some of the drawbacks in this study were the use of DNA as the polyanion and HUVECs. DNA is susceptible to enzymatic degradation and HUVECs exhibit significantly different phenotypic characteristics in comparison to LSECs.

We report the assembly of liver-mimetic architectures comprised of primary rat hepatocytes and human LSECs with an intermediate PEM comprised of chitosan and hyaluronic acid (HA). Chitosan was selected as the cationic PE due to its compatibility with hepatocytes.[24–26] HA found in the basal membranes of connective tissues is utilized to modify surfaces for the culture of endothelial cells.[27,28] We have measured the shear modulus and viscosity of the hydrated chitosan–HA PEM and have conducted studies that demonstrate that liver-specific functions such as urea and albumin secretion, as well as cytochrome P450 (CYP1A1/2) enzymatic activity are maintained and enhanced in the liver-mimetic cellular architectures.

Materials and Methods

Materials

Dulbecco's modified Eagle's medium (DMEM) containing 4.5 g/L glucose, phosphate-buffered saline (PBS), Earle's balanced salt solution, Hank's buffered salt solution, ethoxy resorufin, penicillin, streptomycin, and trypsin–ethylenediaminetetraacetic acid was obtained from Invitrogen Life Technologies. Type IV collagenase, HEPES (4-[2-hydroxyethyl] piperazine-1-ethanesulfonic acid), glucagon, hydrocortisone, ammonia, dicumarol, sodium dodecyl sulfate (SDS), and hydrogen peroxide were obtained from Sigma-Aldrich. Human LSECs and endothelial cell growth medium and supplements were obtained from ScienCell Research Laboratories. Unless noted, all other chemicals were obtained and used as received from Fisher Scientific.

Methods

Hepatocyte isolation and culture. Primary rat hepatocytes were harvested from female Lewis rats (Harlan) that weighed between 170 and 200 g. A two-step *in situ* collagenase perfusion method was utilized.[3,4] Briefly, animals were anesthetized with 3 L/min of a gas mixture of 3% (v/v) isofluorane/97% oxygen (Veterinary Anesthesia Systems Co.). The liver was perfused through the portal vein with Krebs Ringer Buffer (KRB; 7.13 g/L sodium chloride, 2.1 g/L sodium bicarbonate, 1 g/L glucose, 4.76 g/L HEPES and 0.42 g/L potassium chloride) that contained 1 mM ethylenediaminetetraacetic acid, followed by serial perfusion with a 0.075% w/v and a 0.1% w/v collagenase (Sigma; Type IV) in KRB containing 5 mM calcium chloride. Cell suspensions were filtered through nylon meshes with porosity ranging from 250 to 62 μm (Small Parts Inc.). Hepatocytes were separated using a Percoll (Sigma-Aldrich) density centrifugation technique. In a typical separation procedure, 12.5 mL of cell suspension was added to 10.8 mL of Percoll and 1.2 mL of 10× Hank's buffered salt solution, and the resultant mixture was subjected to centrifugation. The cell pellet at the bottom was the hepatocyte fraction, and the supernatant contained the nonparenchymal cell fraction. Hepatocyte viability was determined by trypan blue exclusion. A typical surgical excision and cell isolation typically resulted in 150–200 million hepatocytes with viability ranging from 90% to 97%. Hepatocytes were cultured on collagen-coated six-well sterile tissue culture plates (Becton Dickinson Labware) and were maintained in the culture medium that consisted of DMEM supplemented with 10% heat-inactivated fetal bovine serum (Hyclone), 200 U/mL penicillin, 200 μg/mL streptomycin, 20 ng/mL epidermal growth factor (BD Biosciences), 0.5 U/mL insulin (USP), 14 ng/mL glucagons, and 7.5 μg/mL hydrocortisone. A collagen gelling solution was prepared by mixing nine parts of type I collagen (BD Biosciences) solution and one part of 10× DMEM. Sterile six-well tissue culture plates were coated with 0.5 mL of the gelling solution and incubated at 37°C for 1 h to promote gel formation. Isolated hepatocytes were suspended in the hepatocyte culture medium at a concentration of 1×10^6 cells/mL and seeded on the collagen-coated wells at a density of 1 million cells/well. Collagen sandwich (CS) cultures were formed by the deposition of a second layer of collagen 24 h later. Hepatocytes maintained in stable CS and in unstable confluent monolayer cultures served as positive and negative controls, respectively. Hepatocyte cultures were maintained at 37°C in a humidified gas mixture of 90% air–10% CO_2. The culture medium was replaced every 24 h and medium samples were stored until further analysis.

Assembly of PEMs on hepatocytes. Chitosan (200–300 kDa M.W.; Sigma-Aldrich) and HA (>1 million M.W.; Acros Organics) were used as the cationic and anionic PEs, respectively. Chitosan (0.01%w/v) solutions were prepared by dissolving the polymer in a 1% v/v acetic acid solution and maintained at pH values ranging from 6.1 to 6.3. HA (0.01%w/v) solutions were prepared by diluting in PBS and adjusted to a pH range of 7.2–7.3. PEMs were assembled on hepatocytes by first depositing a cationic PE on the cell layer followed by the anionic PE. The exposure time for each PE solution was ~1–2 min. The desired number of bilayers was obtained through the sequential and alternate deposition of PE layers. At the end of the deposition procedure, the samples were rinsed in 1× PBS and subsequently maintained in the cell culture medium at 37°C. In hepatocyte–PEM only samples, the PEM was deposited after primary hepatocytes were cultured for 24 h.

Hepatocyte–PEM–LSEC cellular constructs. Human LSECs were maintained in a medium supplemented with 5% (v/v) fetal bovine serum, 1% (v/v) endothelial cell growth supplement, 100 U/mL penicillin, and 100 μg/mL streptomycin at 37°C under a humidified gas mixture of 95% air–5% CO_2. Primary hepatocytes were first seeded on collagen-gel-coated surfaces and allowed to spread up to 72 h to form a

confluent layer of cells. Thereafter, a PEM consisting of alternately charged chitosan and HA was deposited, followed immediately by seeding a layer of LSECs. LSECs were plated at a low cell density of 5000 or 10,000 cells per sample since they proliferated over time. Nonadherent LSECs were removed 1 h later. In experiments where the hepatocyte–LSEC or hepatocyte–PEM–LSEC constructs were imaged, the LSECs were tagged with a nontoxic, fluorescent, membrane-permeable dye (PKH 26 Red and Green Fluorescence Cell Linker Kit; Sigma-Aldrich) before seeding. Hepatocyte–LSEC cellular constructs were maintained for up to 10 days in the hepatocyte culture medium. The culture medium was changed every 24 h and medium samples were stored at 4°C until further analysis.

Measurement of the physical properties of the PEM. The self-assembly of hydrated PEMs was monitored *in situ* using a quartz crystal microbalance with dissipation monitoring (QCM-D E4; Q-Sense). The AT-cut quartz crystal coated (Q-Sense) with gold electrodes was cleaned with a 5:1:1 mixture of ammonia, hydrogen peroxide, and 18 MΩ cm PicoPure water (Hydro), respectively. The quartz crystal was excited to its fundamental frequency at ~5 MHz in the QCM-D open module chamber. The PE solution was placed directly on the crystal sensor. The deposition procedures were similar to conditions used to assemble PEMs on live hepatocytes. The change in resonant frequency and the decay time of the vibration relaxations were recorded. The PEM thickness was estimated using the Sauerbrey Equation 1.[29]

$$\Delta f = -\frac{C}{n}\Delta m \tag{1}$$

Δf = change in the resonant frequency (Hz)
Δm = change in mass per unit area (ng/cm^2)
C = sensitivity factor (17.7 Hz · cm^2/ng)
n = overtone number

Since HA and chitosan can also exhibit viscoelastic behavior, the Voigt model (a simple spring and dashpot in parallel operating with no-slip) was applied to the QCM-D response.[30] The change in resonant frequency and change in dissipation factor for a viscoelastic film are related to changes in the resonant frequency and dissipation using Equations 2–4.

$$\Delta f \approx -\frac{1}{2\pi\rho_0 h_0} h\rho\omega\left(1+\frac{2h^2\chi}{3\delta^2(1+\chi^2)}\right) \tag{2}$$

$$\Delta D \approx \frac{2h^3\rho\omega}{3\pi f\rho_0 h_0}\cdot\frac{1}{\delta^2(1+\chi^2)} \tag{3}$$

where ω = angular frequency, h_0 = thickness of the quartz crystal, ρ_0 = density of the quartz crystal, δ = viscous penetration depth, χ = the viscoelastic ratio (ratio of storage to loss moduli), and h and ρ are the thickness and density of the PEM, respectively. The viscoelastic ratio is defined as

$$\chi = \frac{\mu}{\eta\omega} \tag{4}$$

where μ = shear modulus, and η is the film viscosity. The viscoelastic ratio and thickness were varied as the change in frequency, and change in dissipation data were fitted using a mean squared error method.[31,32] Qtools software (Q-Sense) was used to estimate the layer thickness, shear modulus, and viscosity, on the assumption that the density of a PE layer is 1.1 g/cm^3.[23]

Measurement of urea production and albumin secretion. Medium samples were analyzed for rat albumin concentration by an enzyme-linked immunosorbent assay, in triplicate, utilizing a polyclonal antibody to rat albumin (Cappel Laboratories).[23] Urea concentration was determined via its specific reaction with diacetyl monoxime using a commercially available assay kit (BUN Assay Kit; Stanbio Laboratory), with volumes scaled down for use in 96-well plates. The absorbance was measured on a SpectraMax M2 microplate reader (Molecular Devices). Standard curves were generated using purified rat albumin or urea diluted in the culture medium. The data reported were normalized per 1 million cells, which was the initial cell count.

Actin cytoskeletal staining. Hepatocyte cultures were fixed in a 2% glutaraldehyde (Electron Microscopy Sciences) solution in PBS at room temperature for 20 min. The cultures were exposed to a 0.1% Triton X-100 solution to render the membranes permeable and subsequently incubated with rhodamine–phalloidin (Molecular Probes) diluted in a 1% bovine serum albumin in PBS. Actin cytoskeletal structure was imaged using an inverted Zeiss LSM510 confocal microscope (Carl Zeiss Inc.).

Microscopy. Cells were observed and imaged using an inverted Nikon TE-2000 (Nikon) microscope with 10× and 20× objectives. Phase-contrast and fluorescent images of the cells were collected using a Hamamatsu CCD camera and analyzed using Nikon's Imaging Software (NIS-Elements).

Uptake of acetylated low-density lipoprotein by LSECs. Hepatocyte–LSEC cultures were incubated for 3 h with 20 μg/mL of 3,3′-dioctadecylindocarbocyanine (DiI) acetylated low-density lipoprotein (acLdL) (Invitrogen) diluted in the serum-free hepatocyte culture medium. To remove nonspecifically bound acLdL, the cultures were rinsed and maintained in phenol-red-free DMEM. Imaging was conducted on a Nikon TE-2000 microscope.

Di-peptyl peptidase IV immunostaining to image bile canaliculi. Cells were fixed in a 2% glutaraldehyde–PBS solution, followed by permeabilization in a 0.1% Triton X-100 solution. The cultures were incubated overnight at 4°C in a 3% goat serum (Chemicon) solution. The samples were incubated with a mouse monoclonal antibody to rat di-peptyl peptidase IV (Cell Sciences) and a secondary FITC-conjugated rabbit anti-mouse IgG antibody (Sigma-Aldrich) and imaged using an inverted Zeiss LSM510 confocal microscope.

Measurement of cytochrome P450 (CYP1A1/2) activity. Cytochrome P450 (CYP1A1/2) activity was induced by adding 3-methyl cholanthrene (Sigma; 2 μM) to the hepatocyte cultures, 48 h before conducting measurements. Cytochrome-P450-dependent ethoxyresorufin *o*-dealkylase detoxification was measured using ethoxyresorufin as the substrate. The incubation mixture contained the resorufin substrate (5 μM) and 80 μM dicumarol diluted in Earle's

balanced salt solution (Invitrogen).[33] Aliquots (100 μL) were taken at 5, 15, 25, and 35 min after adding the resorufin mixture and transferred to a 96-well plate, and the fluorescence intensity was measured using a SpectraMax M2 microplate reader (excitation wavelength = 530 nm and emission wavelength = 580 nm). Fluorescence intensity was converted to values of concentration by comparison to a standard curve for resorufin fluorescence with concentrations ranging from 0 to 1000 nM. The rate of resorufin formation (nM/min) was calculated from the early linear increase in the fluorescence curve, normalized to the DNA content in hepatocytes, and defined as cytochrome P450 isoenzyme activity. The absolute values obtained on day 7 for CYP1A1/2 activity were divided by the baseline activity on day 1 to obtain values of fold increase.

Separation of hepatocytes and LSECs. The cultures were incubated with a 0.1% w/v collagenase solution. The cell suspensions were incubated with Dynabeads (Dynabeads® CD31 Endothelial Cell; Invitrogen) for 20 min at 4°C in an orbital shaker. Dynabead-bound cells (LSEC fractions) were collected by a magnet (DynaMag™-15; Invitrogen) and the supernatants (hepatocyte fractions) were transferred to a new tube. Purity of cell populations was observed to be >97%. Hepatocyte fractions were centrifuged and diluted in a 0.1% SDS solution for measurement of DNA content.

Measurement of DNA content. Cells were harvested by treatment with a 0.1% collagenase solution and subsequently lysed in a 0.1% SDS solution and stored at −20°C until further analysis. For DNA measurements, aliquots of cell suspensions were treated with a fluorescent DNA-binding dye (Hoechst 33258, pentahydrate-*bis*-benzimide; Invitrogen). Fluorescence intensity was measured using a SpectraMax M2 microplate reader (excitation and emission wavelengths were 355 and 460 nm, respectively). Fluorescence intensity was converted to DNA concentration by comparison to a standard curve for calf thymus DNA (Sigma-Aldrich) fluorescence with concentrations ranging from 0 to 40 μg/mL.

Statistical analysis. All data are reported as mean ± standard deviation. *t*-tests were conducted to detect differences in the mean values ($\alpha = 0.05$). The Bonferroni correction was used to account for multiple hypothesis testing. The corrected *p*-values are reported.

Results

PEMs comprised of 5 up to 30 alternating layers of chitosan and HA were assembled above a confluent layer of primary hepatocytes. The height of the hydrated PEM as well as its modulus and viscosity were determined by QCM-D measurements.[29,31,32] The film thickness, shear modulus, and visocosity of each layer were modeled by following an iterative method using the Voigt model approximation[30] (Table 1). The thickness was found to be ~6 nm/PE layer for a PEM consisting of five layers. The thickness per PE layer reached a maximum value of 5.2 nm/layer for a PEM of 10 layers. While the reason for the sub-linear growth of film thickness with layer number in the present case is not completely clear, it may be due to the fact that the chitosan was not highly charged at the pH at which it was deposited. The values for shear modulus were initially high due to substrate effects (95.7 ± 66.3 kPa for five layers) but decreased as more layers were deposited before increasing again to reach a maximum value (104.5 ± 13.6 kPa) for a PEM comprised of 15 bilayers. The PEM exhibited viscoelastic characteristics and was found to be less rigid as more layers were deposited. The PEM film viscosity values were found to be similar to that of water (1.01 mPas), indicating a high degree of hydration.[34]

Table 1. Thickness, Shear Modulus, and Viscosity Values for Hydrated Chitosan–Hyaluronic Acid Polyelectrolyte Multilayers

Layer	*Thickness (nm)*	*Shear modulus (kPa)*	*Film viscosity (mPas)*
5	30.82 ± 6.71	95.7 ± 66.3	1.69 ± 0.18
10	52.27 ± 5.25	56.6 ± 17.8	1.78 ± 0.09
15	55.50 ± 4.18	104.5 ± 13.6	2.12 ± 0.09

In the first step toward assembling 3D liver mimics, hepatocyte–PEM cultures were investigated. Urea production and albumin secretion were measured to evaluate the phenotypic function and the results were compared to CS cultures (positive control) and hepatocyte monolayers (negative control) (Fig. 1). Over a 7-day period, urea production decreased by 64% and 33% for hepatocyte monolayer and CS cultures, respectively. Urea production was observed to be lower in cultures with PEMs than in hepatocytes cultured as a monolayer or CS samples on day 1. This was attributed to the fact that hepatocytes that undergo PEM deposition take ~2 days to stabilize from the deposition procedure; however, these cells exhibited increased urea production over the culture period. The increase in urea production was found to be 12% and 48% for hepatocyte cultures that had either 5 or 15 PE layers, respectively. The values for urea production on day 7 were higher and statistically significant ($p < 0.05$) in hepatocyte cultures with 5 (49.1 ± 4.4 μg/10^6 hepatocytes,

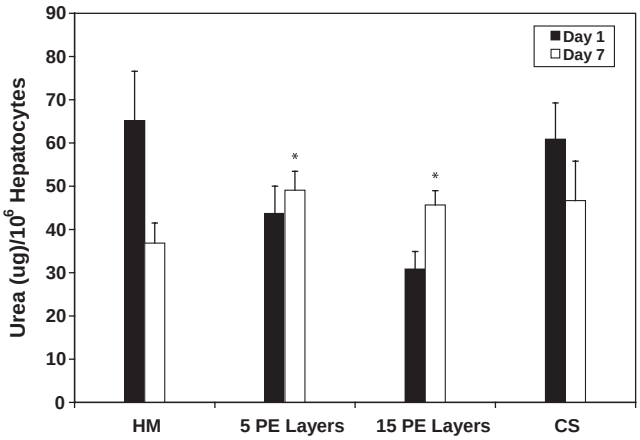

FIG. 1. Urea production measured over a 7-day period for HM ($n = 6$), with 5 PE layers (5 PE layers, $n = 6$), with 15 PE layers (15 PE layers, $n = 6$), and in a CS ($n = 6$). *$p < 0.05$ when compared to hepatocyte monolayers on day 7. CS, collagen sandwich; HM, hepatocytes cultured as a monolayer.

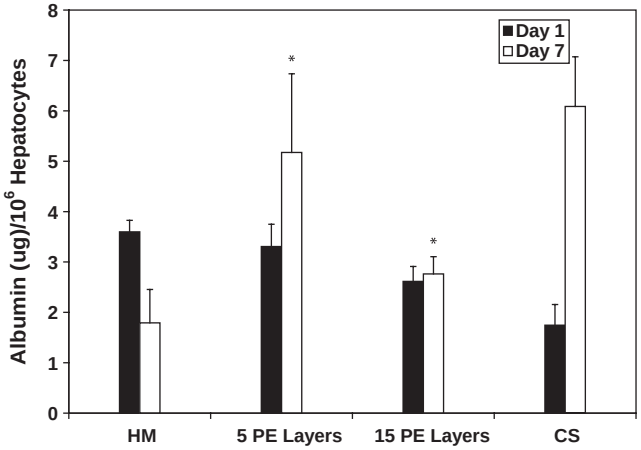

FIG. 2. Albumin production measured over a 7-day period for HM ($n=6$), with 5 PE layers (5 PE layers, $n=6$), with 15 PE layers (15 PE layers, $n=6$), and in a CS ($n=6$). *$p<0.05$ when compared to hepatocyte monolayers on day 7.

$p=0.0016$) or 15 ($45.7\pm3.3\,\mu g/10^6$ hepatocytes, $p=0.008$) PE layers in comparison to hepatocyte monolayer ($36.8\pm4.6\,\mu g/10^6$ hepatocytes) and were similar and statistically insignificant ($p>0.05$) in comparison to values measured for CS ($46.7\pm9.1\,\mu g/10^6$ hepatocytes) cultures. In stable hepatocyte cultures, albumin secretion has been shown to increase with time.[3,4] Over a 7-day period, albumin secretion increased by 71% in CS cultures and decreased by 50% in monolayer cultures (Fig. 2). Albumin secretion in hepatocyte–PEM cultures increased over the 7-day observation period. In hepatocyte cultures with 5 or 15 PE layers, albumin secretion increased by $\sim$36% or 7%, respectively. Cultures with PEMs consisting of 30 or 45 PE layers did not exhibit satisfactory urea or albumin production and were not included in further analyses. The values for albumin secretion on day 7 were higher and statistically significant ($p<0.05$) in hepatocyte cultures with 5 ($5.2\pm1.6\,\mu g/10^6$ hepatocytes, $p=0.003$) or 15 PE layers ($2.8\pm0.3\,\mu g/10^6$ hepatocytes, $p=0.0024$) in comparison to hepatocyte monolayers ($1.8\pm0.7\,\mu g/10^6$ hepatocytes) and were similar and statistically insignificant ($p>0.05$) in comparison to values measured for CS ($6.1\pm0.9\,\mu g/10^6$ hepatocytes) cultures.

The actin cytoskeletal organization revealed significant differences between hepatocyte monolayers and hepatocyte–PEM cultures. In the absence of rhodamine phalloidin, fluorescence was not observed in hepatocytes, and this was defined as the negative control (Fig. 3A). Hepatocyte monolayer cultures exhibited a mesh-like network of f-actin through the entire cross section of the cell (Fig. 3B). The cytoskeletal organization in hepatocyte–PEM samples was observed to be very similar to hepatocytes cultured in a CS culture (Fig. 3C). In these cells, f-actin was observed to be localized only along the peripheral regions of the cell similar to hepatocytes cultured in a CS.

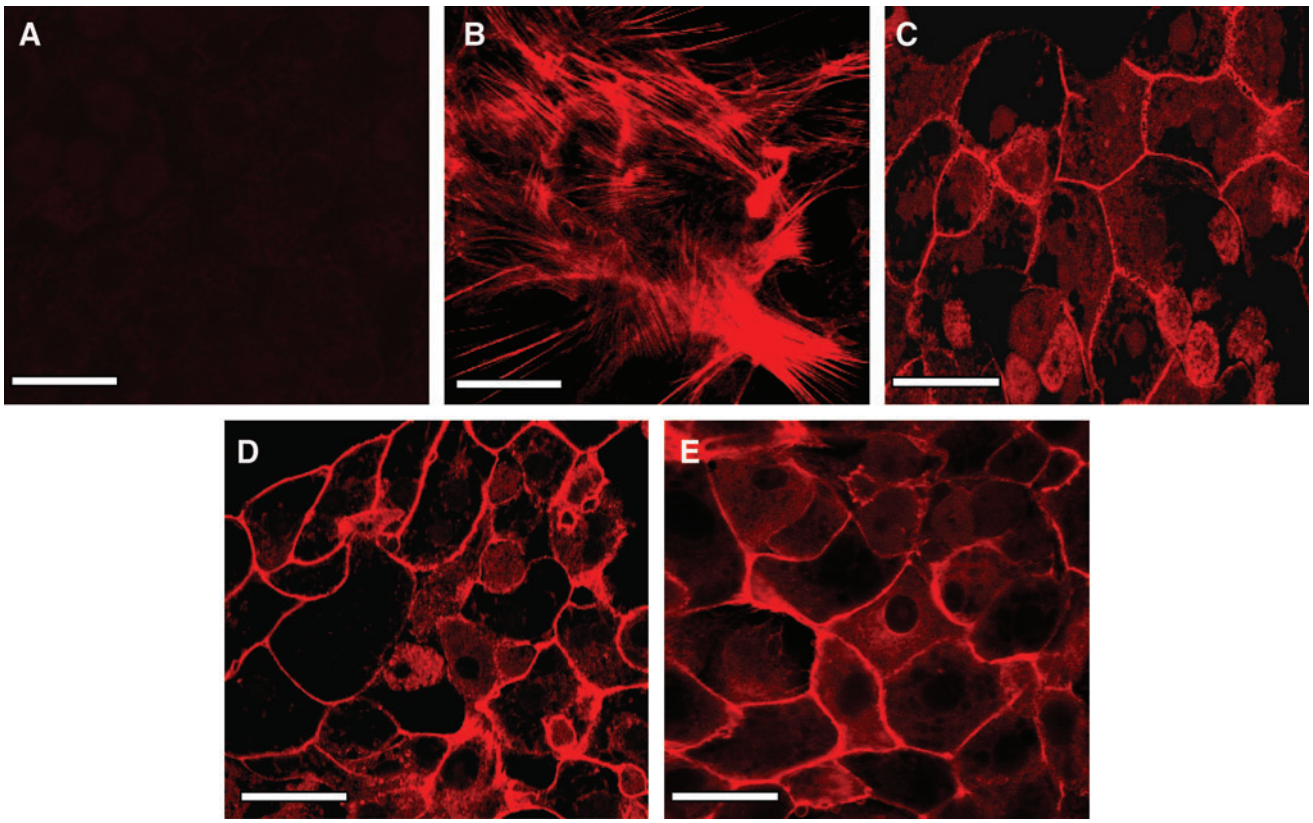

FIG. 3. Actin cytoskeletal organization in (**A**) Hepatocyte monolayer without the addition of rhodamine phalloidin (negative control), (**B**) Hepatocyte monolayer, (**C**) CS culture, (**D**) Hepatocytes–5PE Layers, and (**E**) Hepatocytes–15 PE Layers. Scale bar = 50 μm. Color images available online at www.liebertonline.com/ten.

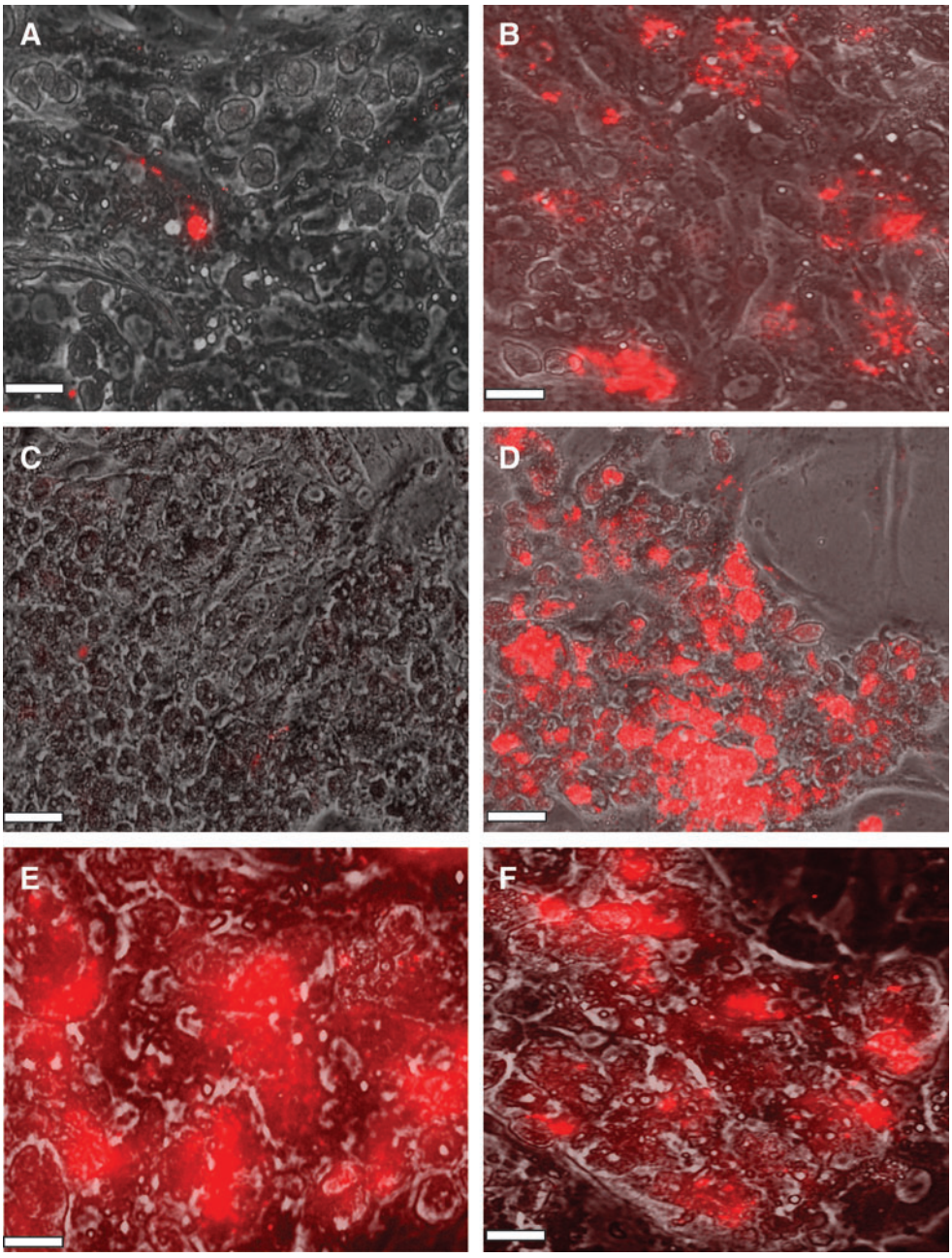

FIG. 4. Merged phase-contrast (hepatocytes) and red-fluorescent LSECs. Images taken 2 h post-LSEC seeding. (**A**) Hepatocytes–LSECs and (**B**) Hepatocytes-5 PE Layers–5000 LSECs. Merged phase-contrast (hepatocytes) and fluorescent (LSECs) images taken 7 days post-LSEC seeding. (**C**) Hepatocytes–LSECs, (**D**) Hepatocytes–5 PE Layers–5000 LSECs, (**E**) Hepatocytes–5 PE Layers–10,000 LSECs, and (**F**) Hepatocytes–15 PE Layers–5000 LSECs. Scale bar = 100 μm. LSEC, liver sinusoidal endothelial cell.

A second layer of LSECs was deposited on hepatocyte–PEM cultures as well as on hepatocyte monolayers (Fig. 4). Images taken 2 h post-LSEC seeding indicated that in the absence of an intermediate PE scaffold, LSECs were nonadherent (Fig. 4A). However, in the presence of the chitosan–HA PEM, LSECs were adherent (Fig. 4B). These trends prevailed over longer culture periods as well, suggesting that the PEM provides a biocompatible surface for LSECs to adhere and proliferate. On day 7, in the absence of the chitosan–HA scaffold, LSECs were not observed above hepatocytes (Fig. 4C), whereas high concentrations of LSECs were observed on hepatocyte–PEM–LSEC constructs (Fig. 4D–F). It is significant to note that LSECs appeared to be adherent only above hepatocytes and were not found in regions between adjacent hepatocyte aggregates (Fig. 4D–F). The maintenance of LSEC phenotype was assessed by fluorescent imaging of the receptor-mediated uptake of acLdL. In the absence of acLdL, no fluorescence was observed in LSECs or hepatocytes (Fig. 5A, B). Since hepatocytes do not have this receptor, these cells did not exhibit any fluorescence (Fig. 5C, D) as well as

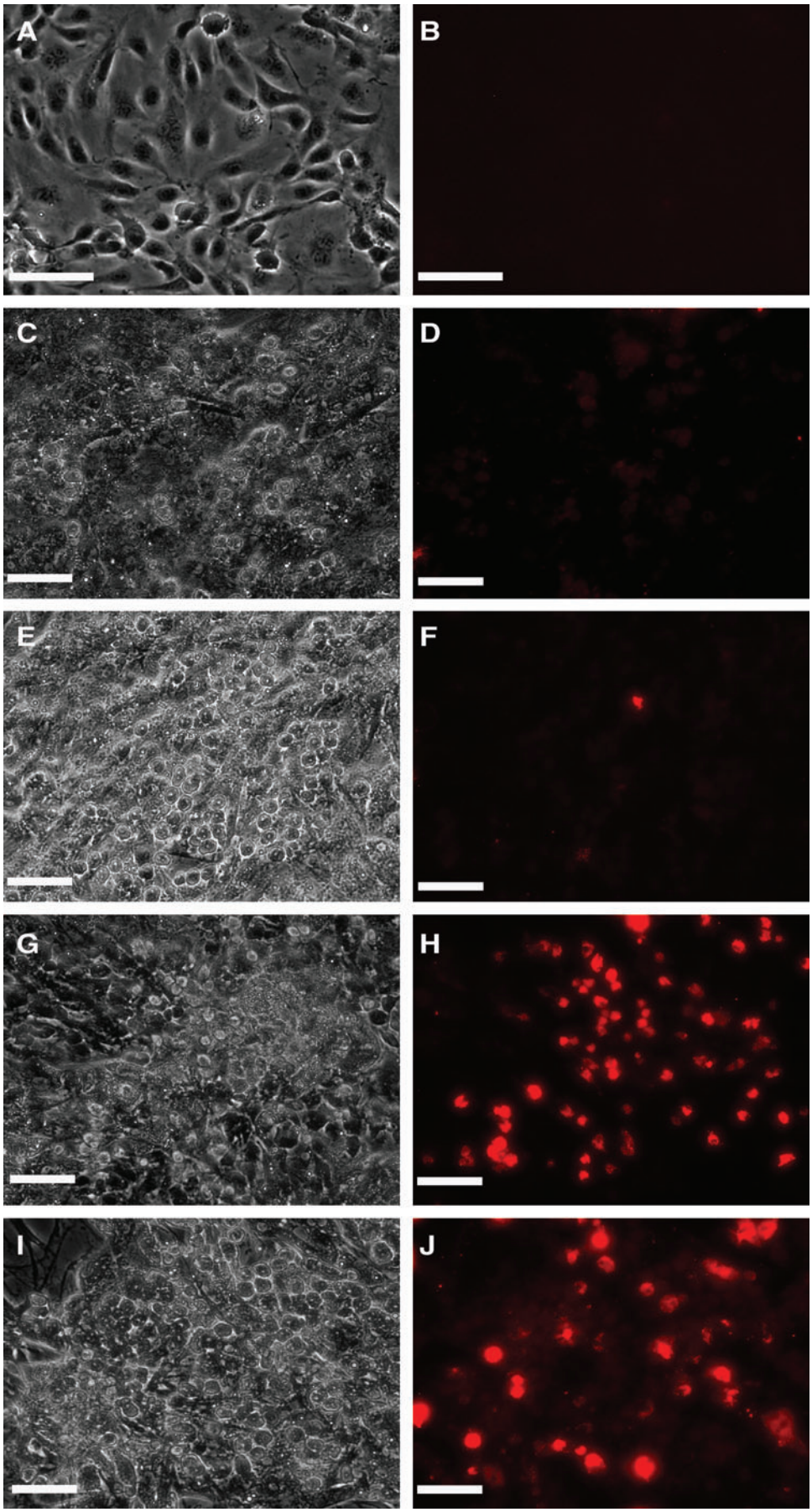

FIG. 5. Phase-contrast images of (**A**) LSECs, (**C**) Hepatocytes, (**E**) Hepatocyte–LSECs, (**G**) Hepatocytes–5 PE Layers–5000 LSECs, and (**I**) Hepatocytes–15 PE Layers–5000 LSECs. Fluorescent images of acetylated low-density lipoprotein uptake for (**B**) LSECs (negative control, in the absence of acetylated low-density lipoprotein), (**D**) Hepatocytes, (**F**) Hepatocytes–LSECs, (**H**) Hepatocytes–5 PE Layers–5000 LSECs, and (**J**) Hepatocytes–15 PE Layers–5000 LSECs. Scale bar = 100 μm. Color images available online at www.liebertonline.com/ten.

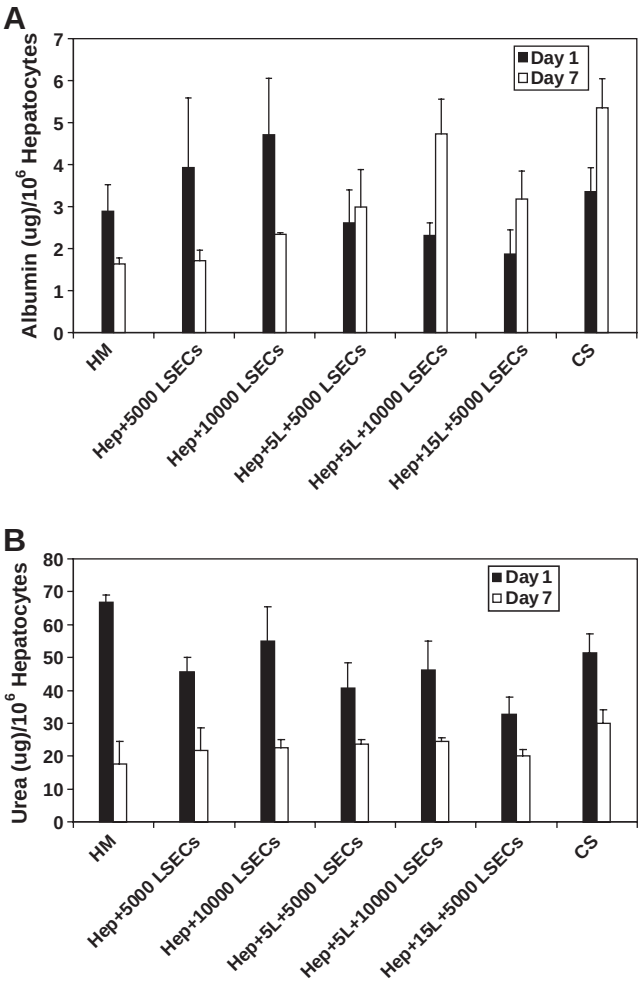

FIG. 6. Albumin secretion (**A**) and urea production (**B**) measured over a 7-day period for HM, with LSECs in the absence of a PEM (Hep + 5000 LSECs and Hep + 10,000 LSECs), with LSECs in the presence of a PEM (Hep + 5L 5000 LSECs, Hep + 5L + 10,000 LSECs, and Hep + 15L 5000 LSECs) and in a CS ($n = 3$ for all conditions). PEM, polyelectrolyte multilayer.

LSECs cultured on hepatocytes in the absence of a PEM (Fig. 5E, F). However, LSECs adherent on hepatocyte–PEM samples exhibited fluorescence, indicating the endocytosis of the low-density lipoprotein (Fig. 5G–J). These results indicate that LSEC phenotype is maintained in the 3D constructs.

On day 7 (Fig. 6A), albumin secretion in hepatocyte–PEM–LSEC cultures was statistically higher ($p < 0.05$) in comparison to hepatocyte monolayers. The p-values for hepatocyte–5L–5000 LSECs, hepatocyte–5L–10,000 LSECs, and hepatocyte–15L–5000 LSECs were found to be 0.04, 0.006, and 0.015, respectively. Samples containing LSECs in the presence of a PE interface exhibited statistically higher albumin secretion compared with hepatocyte–LSEC cultures. The p-values for hepatocyte–5L–10,000 LSECs and hepatocyte–15L–5000 LSECs were found to be 0.039 and 0.03, respectively, when compared to albumin production in the absence of a PE multilayer. However, the albumin secretion for all 3D liver mimics was found to be similar to CS cultures and the values were statistically insignificant. Urea production decreased over the 7-day period for all samples. Hepatocytes cultured as a monolayer samples exhibited ~70% decrease in urea production over a 7-day period (Fig. 6B). The decrease in the hepatocyte–PEM–LSEC samples was ~40%–45% and similar to the decrease observed in CS cultures.

An important differentiated function of hepatocytes is the presence of bile canaliculi, the channels through which bile acids are transported from the liver.[35,36] The presence of canaliculi was determined through the localization of a fluorescent di-peptyl peptidase IV enzyme. Very diffuse fluorescence was observed in hepatocyte monolayers and hepatocyte–LSEC cultures (Fig. 7C, D), indicating that well-defined canaliculi were not formed. These structures were better defined in hepatocyte–PEM cultures (Fig. 7E). However, well-defined bile canaliculi were observed in hepatocyte–PEM–LSEC (Fig. 7F, G) and CS cultures (Fig. 7B). These results suggest that the PEM plays an important role in maintaining cellular polarity and in modulating the heterotypic interactions between hepatocytes and LSECs.

CYP1A1/2 isoenzyme activity was monitored over a 7-day period since the metabolism of toxins, an important phenotypic function of hepatocytes, is mediated through the CYP class of microsomal enzymes. Control measurements conducted on LSEC cultures revealed that LSECs exhibited extremely low enzymatic activity. For example on day 1, the CYP1A1/2 activity for LSECs was found to be 0.12 ± 0.03 nM/min/μg DNA in comparison to the activity in a CS culture (4.14 ± 0.4 nM/min/μg DNA). On day 7, the values were found to be 0.06 ± 0.02 and 8.45 ± 1.6 nM/min/μg DNA for LSECs and CS cultures, respectively. Since the enzymatic activity on day 7 exhibited by hepatocytes alone is ~140 times higher than that observed for LSECs alone, we concluded that the CYP enzyme activity observed in the 3D constructs is primarily due to hepatocytes. The CYP1A1/2 activity remained stable in hepatocyte–PEM samples and exhibited a twofold increase in CS cultures. A significant increase was observed only in hepatocyte–PEM–LSEC constructs where the fold increase over the observation period ranged from 4-fold to 16-fold (Fig. 8). Three-dimensional liver mimics that contained 10,000 of LSECs exhibited either a 7.5-fold (hepatocyte–5 PE Layers–10,000 LSECs) or a 16-fold increase (hepatocyte–15 PE Layers–10,000 LSECs) These trends suggest that the communications and interactions between these two cells types are critical for enhancing the detoxification capability of hepatocytes *in vitro*.

Discussion and Conclusions

The design of 3D structures of hepatic parenchymal and nonparenchymal cells using PE scaffolds is an innovative approach to mimic liver sinusoidal structure found *in vivo*. Although hepatocytes cultured in a CS configuration are stable over extended periods of time, they do not resemble liver architecture *in vivo*. Additionally, the presence of thick collagen gels prevents the assembly of 3D stratified cellular constructs. LSECs have been shown to function as a scavenger system *in vivo*, by playing a vital role in the balance of lipids, cholesterol, and vitamins.[37–41] Through blood clearance, LSECs can remove waste macromolecules that are either soluble or colloidal in nature. Several components of connective tissue are eliminated rapidly from the blood through receptor-mediated endocytosis in LSECs.

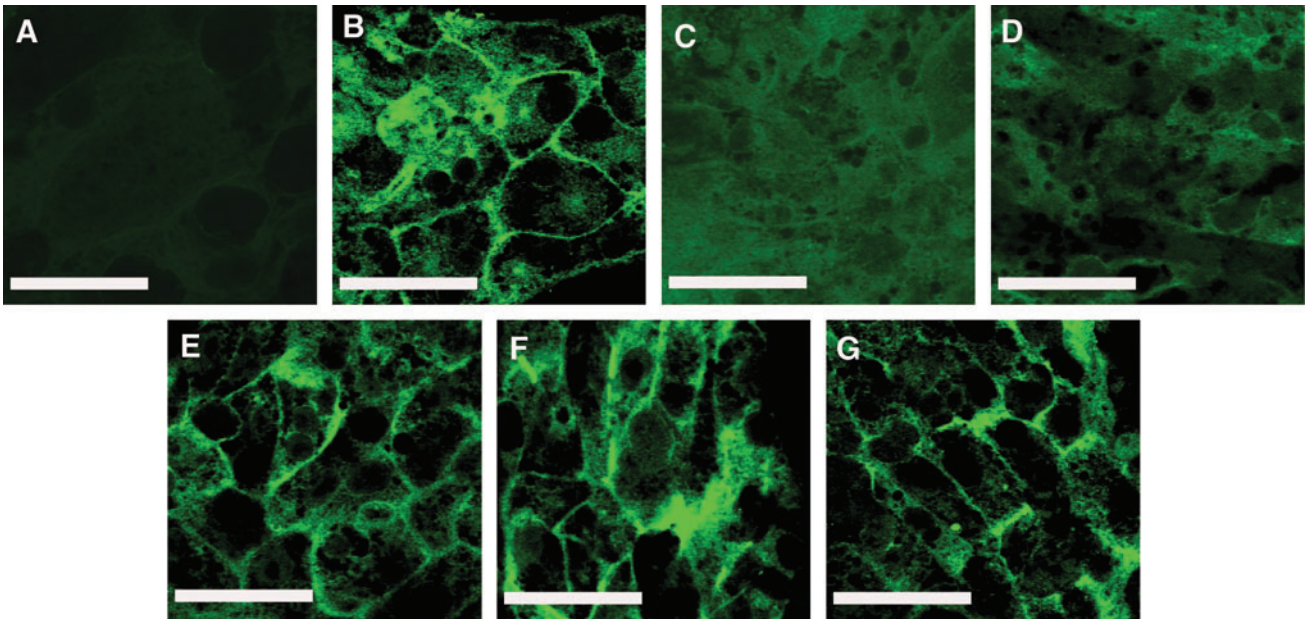

FIG. 7. Di-peptyl peptidase IV immunostaining for bile canaliculi measured 3 days post-LSEC seeding. (**A**) Negative control (CS culture in the absence of antibodies), (**B**) CS culture, (**C**) Hepatocyte Monolayer, (**D**) Hepatocytes + 5000 LSECs, (**E**) Hepatocytes + 15 PE layers, (**F**) Hepatocytes + 15 PE + 5000 LSECs, and (**G**) Hepatocytes + 15 PE + 10,000 LSECs. Scale bar = 50 μm.

Chitosan–HA PEMs exhibited shear modulus values that are in the range reported for the bulk modulus values of the liver.[42,43] PEMs exhibiting elastic moduli in the 100 kPa range have been shown to maintain and modulate hepatic phenotype, suggesting that the shear modulus values reported in this study are suitable for the assembly of liver sinusoidal mimics.[44] The films are well hydrated, thereby promoting the diffusion of small molecules such as cytokine and other signaling molecules. Hepatocyte–PEM cultures with either 5 or 15 PE layers were found to exhibit urea and albumin production similar to CS cultures. This is of importance because the height of the PEM ranges from 30 to 55 nm, which is significantly lower than the thickness of a collagen gel (in the mm range). It is hypothesized that the height of the PEM decreases slightly due to the formation of chitosan aggregates.[45,46] These data suggest that cellular polarization, an important feature of hepatocytes cultured in CS cultures, occurs even in the presence of a nano-scale PEM. Further, the nano-scale dimensions of the PEM offer the potential to promote and control homotypic and heterotypic cellular interactions.

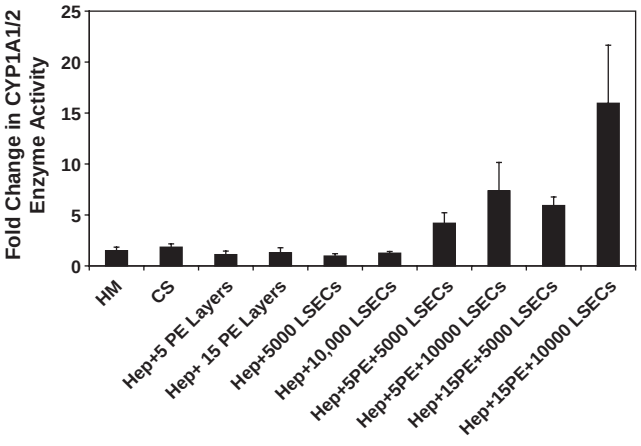

FIG. 8. Fold change in CYP1A1/2 enzyme activity for HM and CS, with PEMs only, with LSECs only, and in three-dimensional liver mimics ($n = 3$ for all conditions).

The chitosan–HA PEM provides a surface for LSECs to adhere and proliferate. LSECs were found to adhere only on hepatocytes in the presence of a PEM and were nonadherent in the absence of PEMs or in regions adjacent to hepatocyte aggregates. Hepatic phenotypic features such as bile canaliculi were well defined in hepatocyte–PEM–LSEC samples in comparison to hepatocyte monolayers or hepatocyte–LSEC cultures, thereby suggesting enhanced autocrine/paracrine signaling through the PEM. Cytochrome P450, CYP1A1/2 activity was enhanced up to 16-fold over a 7-day period in hepatocyte–PEM–LSEC cultures. These observations suggest that the hepatocyte–PEM–LSEC constructs could provide a more physiologically relevant model system to study the metabolism of drugs and toxins. In the future, our goal is to investigate the enzyme kinetics of CYP3A, which accounts for the metabolism of ~50% of pharmaceuticals available today,[47,48] as well as the CYP2B and CYP2C family of enzymes, implicated in the metabolism of amphetamines and anti-inflammatory agents.[49,50] The modes through which hepatic parenchymal and nonparenchymal cells communicate remain cryptic. Through detailed studies on profiling cytokine levels as well through gene expression studies, our future goals are to unearth molecular signatures and the key signaling molecules that enhance cell–cell communications in hepatic architectures.

Some alternate approaches to design hepatic structures are the use of a temperature-responsive polymer such as *N*-isopropyl acrylamide,[17–19] the use of cationic magnetic liposome,[20] and the use of laser guided writing techniques.[51,52]

In the first two approaches, issues related to working with cell sheets and the long-term effects of magnetic liposomes pose problems. Although laser-guided writing techniques are a promising approach, the design of large 3D liver models could potentially be time consuming. More recently, studies on perfused cocultures of primary hepatocytes and LSECs reveal that such systems can maintain LSEC phenotype.[37] Our approach to design 3D liver mimics through the incorporation of PEMs and hepatic cells is a simple and effective methodology. The PEMs used in this study are biocompatible and biodegradable and do not affect hepatic phenotype. In the future, the PEMs can be modified with hepatocyte-specific adhesive ligands to promote receptor-mediated adhesion. Cellular constructs that mimic liver sinusoidal structure *in vivo* could aid in the design of liver-assist devices and provide accurate models for applications in toxicity and drug testing. Since LSECs are the first barrier to blood-borne pathogens in the liver, tissue mimics that incorporate these cells could play a vital role in advancing our knowledge on the communications and signaling between hepatic parenchymal and nonparenchymal cells.

Acknowledgments

We gratefully acknowledge financial support from the National Institutes of Health (NIDDK-1R21DK077802, P.R.), the National Science Foundation (DMR-090750, P.R. and R.M.D.), Thomas F. and Kate Miller Jeffress Foundation (P.R.), the Institute for Critical Technology and Applied Sciences (P.R.), and the MILES-NSF IGERT program at Virginia Polytechnic Institute and State University (P.R.).

Disclosure Statement

No competing financial interests exist.

References

1. Arias, I.M., Boyer, J.L., Chisari, F.V., Fausto, M., Schachter, D., and Shafritz, D.A. The Liver: Biology and Pathology, 4th edition. Philadelphia, PA: Lippincott Williams and Wilkins, 2001.
2. Sechser, A., Osorio, J., Friese, C., and Osorio, R.W. Artificial liver support devices for fulminant liver failure. Clin Liver Dis **5,** 415, 2001.
3. Dunn, J.C.Y., Yarmush, M.L., Koebe, H.G., and Tompkins, R.G. Hepatocyte function and extracellular matrix geometry: long-term culture in a sandwich configuration. FASEB J **3,** 174, 1989.
4. Dunn, J.C.Y., Tompkins, R.G., and Yarmush, M.L. Long-term *in vitro* function of adult hepatocytes in a collagen sandwich configuration. Biotechnol Prog **7,** 237, 1991.
5. Kuri-Harcuch, W., and Mendoza-Figueroa, T. Cultivation of adult rat hepatocytes on 3T3 cells: expression of various liver differentiated functions. Differentiation **41,** 148, 1989.
6. Bhatia, S.N., Yarmush, M.L., and Toner, M. Controlling cell interactions by micropatterning in co-cultures: hepatocytes and 3T3 fibroblasts. J Biomed Mater Res **34,** 189, 1997.
7. Bhatia, S.N., Balis, U.J., Yarmush, M.L., and Toner, M. Effect of cell-cell interactions in preservation of cellular phenotype: cocultivation of hepatocytes and nonparenchymal cells. FASEB J **13,** 1883, 1999.
8. Corlu, A., Ilyin, G., Cariou, S., Lamy, I., Loyer, P., and Guguen-Guilluozo, C. The coculture: a system for studying the regulation of liver differentiation/proliferation activity and its control. Cell Biol Toxicol **13,** 235, 1997.
9. Khetani, S.R., Szulgit, G., Del Rio, J.A., Barlow, C., and Bhatia, S.N. Exploring interactions between rat hepatocytes and nonparenchymal cells using gene expression profiling. Hepatology **40,** 545, 2004.
10. Tilles, A.W., Baskaran, H., Roy, P., Yarmush, M.L., and Toner, M. Effects of oxygenation and flow on the viability and function of rat hepatocytes co-cultured in a microchannel flat-plate bioreactor. Biotechnol Bioeng **73,** 379, 2001.
11. Zaret, K.S. Regulatory phases of early liver development: paradigms of organogenesis. Nat Rev Genet **3,** 499, 2002.
12. Cleaver, O., and Melton, D.A. Endothelial signaling during development. Nat Med **9,** 661, 2003.
13. Matsumoto, K., Yoshitomi, H., Rossant, J., and Zaret, K.S. Liver organogenesis promoted by endothelial cells prior to vascular function. Science **294,** 559, 2001.
14. Ross, M.A., Sander, C.M., Kleeb, T.B., Watkins, S.C., and Stolz, D.B. Spatiotemporal expression of angiogenesis growth factor receptors during the revascularization of regenerating rat liver. Hepatology **34,** 1135, 2001.
15. Nahmias, Y., Casali, M., Barbe, L., Berthiaume, F., and Yarmush, M.L. Liver endothelial cells promote LDL-R expression and the uptake of HCV-like particles in primary rat and human hepatocytes. Hepatology **43,** 257, 2006.
16. Nahmias, Y., Schwartz, R.E., Hu, W.-S., Verfaillie, C.M., and Odde, D.J. Endothelium-mediated hepatocyte recruitment in the establishment of liver-like tissue *in vitro*. Tissue Eng **12,** 1627, 2006.
17. Harimoto, M., Yamato, M., Hirose, M., Takahashi, C., Isoi, Y., Kikuchi, A., and Okano, T. Novel approach for achieving double-layered cell sheets co-culture: overlaying endothelial cell sheets onto monolayer hepatocytes utilizing temperature-responsive culture dishes. J Biomed Mater Res **62,** 464, 2002.
18. Shimizu, T., Yamato, M., Kikuchi, A., and Okano, T. Cell sheet engineering for myocardial tissue reconstruction. Biomaterials **24,** 2309, 2003.
19. Shimizu, T., Yamato, M., Isoi, Y., Akutsu, T., Setomaru, T., Abe, K., Kikuchi, A., Umezu, M., and Okano, T. Fabrication of pulsatile cardiac tissue grafts using a novel 3-dimensional cell sheet manipulation technique and temperature-responsive cell culture surfaces. Circ Res **90,** e40, 2002.
20. Ito, A., Takizawa, Y., Honda, H., Ken-ichiro Hata, K.-I., Kagami, H., Ueda, M., and Kobayashi, T. Tissue engineering using magnetite nanoparticles and magnetic force: heterotypic layers of cocultured hepatocytes and endothelial cells. Tissue Eng **10,** 833, 2004.
21. Wilson, C.W., and Boland, T. Cell and organ printing 1: protein and cell printers. Anat Rec Part A **272A,** 491, 2003.
22. Boland, T., Mironov, V., Gutowska, A., Roth, E.A., and Markwald, R.R. Cell and organ printing 2: fusion of cell aggregates in three-dimensional gels. Anat Rec Part A **272A,** 497, 2003.
23. Rajagopalan, P., Shen, C.J., Berthiaume, F., Tilles, A.W., Toner, M., and Yarmush, M.L. Polyelectrolyte nanoscaffolds for the design of layered cellular architectures. Tissue Eng **12,** 1553, 2006.
24. Chung, T.W., Yang, J., Akaike, T., Cho, K.Y., Nah, J.W., Kim, S.I., and Cho, C.S. Preparation of alginate/galactosylated chitosan scaffold for hepatocyte attachment. Biomaterials **23,** 2827, 2002.
25. Park, I.-K., Yang, J., Jeong, H.-J., Bom, H.-S., Harada, I., Akaike, T., Kim, S.-I., and Cho, C.-S. Galactosylated chitosan

as a synthetic extracellular matrix for hepatocytes attachment. Biomaterials **24,** 2331, 2003.
26. Park, I.K., Kim, T.H., Park, Y.H., Shin, B.A., Choi, E.S., Chowdhury, E.H., Akaike, T., and Cho, C.S. 2001. Galactosylated chitosan-graft-poly(ethylene glycol) as hepatocyte-targeting DNA carrier. J Controlled Release **76,** 349, 2001.
27. Joddar, B., and Ramamurthi, A. Elastogenic effects of exogenous hyaluronan oligosaccharides on vascular smooth muscle cells. Biomaterials **27,** 5698, 2006.
28. Remuzzi, A., Mantero, S., Colombo, M., Morigi, M., Binda, E., Camozzi, D., and Imberti, B. Vascular smooth muscle cells on hyaluronic acid: culture and mechanical characterization of an engineered vascular construct. Tissue Eng **10,** 699, 2004.
29. Sauerbrey, G. Verwendung von Schwingquarzen zur Wägung Dünner Schichten und zur Mikrowägung. Z Phys A At Nucl **155,** 206, 1959.
30. Voinova, M.V., Rodahl, M., Jonson, M., and Kasemo, B. Viscoelastic acoustic response of layered polymer films at fluid-solid interfaces: continuum mechanics approach. Phys Scr **59,** 391, 1999.
31. de Kerchove, A.J., and Elimelech, M. Formation of polysaccharide gel layers in the presence of Ca2+ and K+ ions: measurements and mechanisms. Biomacromolecules **8,** 113, 2007.
32. Munro, J.C., and Frank, C.W. Polyacrylamide adsorption from aqueous solutions on gold and silver surfaces monitored by the quartz crystal microbalance. Macromolecules **37,** 925, 2004.
33. Behnia, K., Bhatia, S.N., Jastromb, N., Balis, U., Sullivan, S., Yarmush, M.L., and Toner, M. Xenobiotic metabolism by cultured primary hepatocytes. Tissue Eng **6,** 467, 2000.
34. Green, D.W., and Perry, R.H. Perry's Chemical Engineers' Handbook, 8th edition. New York, NY: McGraw-Hill, 2008.
35. Khetani, S.R., and Bhatia, S.N. 2008. Microscale culture of human liver cells for drug development. Nat Biotechnol **26,** 120, 2008.
36. Liu, X., LeCluyse, E.L., Brouwer, K.R., Gan, L.-S.L., Lemasters, J.J., Stieger, B., Meier, P.J., and Brouwer, K.L.R. Biliary excretion in primary rat hepatocytes cultured in a collagen sandwich configuration. Am J Physiol Gastrointest Liver Physiol **277,** G12, 1999.
37. Hwa, A.J., Fry, R.C., Sivaraman, A., So, P.T., Samson, L.D., Stolz, D.B., and Griffith, L.G. Rat liver sinusoidal endothelial cells survive without exogenous VEGF in 3D perfused cocultures with hepatocytes. FASEB J **21,** 2564, 2007.
38. Smedsrød, B., Melkko, J., Araki, N., Sano, H., and Horiuchi, S. Advanced glycation end products are eliminated by scavenger-receptor mediated endocytosis in hepatic sinusoidal Kupffer and endothelial cells. Biochem J **322,** 567, 1997.
39. Seternes, T., Sørensen, K., and Smedsrød, B. Scavenger endothelial cells of vertebrates: a nonperipheral leukocyte system for high-capacity elimination of waste macromolecules. Proc Natl Acad Sci USA **99,** 7594, 2002.
40. Elvevold, K.H., Geir I Nedredal, G.I., Revhaug, A., and Smedsrød, B. Scavenger properties of cultivated pig liver endothelial cells. Comp Hepatol **3,** 4, 2004.
41. Smedsrød, B. Clearance function of scavenger endothelial cells. Comp Hepatol **3,** S22, 2004.
42. Nava, A., Mazza, E., Furrer, M., Villiger, P., and Reinhart, W.H. *In vivo* mechanical characterization of human liver. Med Image Anal **12,** 203, 2008.
43. Sandrin, L., Fourquet, B., Hasquenoph, J.M., Yon, S., Fournier, C., Mal, F., Christidis, C., Ziol, M., Poulet, B., Kazemi, F., Beaugrand, M., and Palau, R. Transient elastography: a new noninvasive method for assessment of hepatic fibrosis. Ultrasound Med Biol **29,** 1705, 2003.
44. Chen, A.A., Khetani, S.R., Lee, S., Bhatia, S.N., and Van Vliet, K.J. Modulation of hepatocyte phenotype *in vitro* via chemomechanical tuning of polyelectrolyte multilayers. Biomaterials **30,** 1113, 2009.
45. Pa, J., and Yu, T.L. Light scattering study of chitosan in acetic acid aqueous solutions. Macromol Chem Phys **202,** 985, 2001.
46. Lee, S.B., Lee, Y.M., Song, K.W., and Park, M.H. Preparation and properties of polyelectrolyte complex sponges composed of hyaluronic acid and chitosan and their biological behaviors. J Appl Polym Sci **90,** 925, 2003.
47. Omiecinski, C.J., Remmel, R.P., and Hosagrahara, V.P. Concise review of the cytochrome P450s and their roles in toxicology. Toxicol Sci **48,** 151, 1999.
48. Thummel, K.E., and Wilkinson, G.R. *In vitro* and *in vivo* drug interactions involving human CYP3A. Annu Rev Pharmacol Toxicol **38,** 389, 1998.
49. Rendic, S., and Di Carlo, F.J. Human cytochrome P450 enzymes: a status report summarizing their reactions, substrates, inducers, and inhibitors. Drug Metab Rev **29,** 413, 1997.
50. Rahman, A., Korzekwa, K.R., Grogan, J., Gonzalez, F.J., and Harris, J.W. Selective biotransformation of taxol to 6 alpha-hydroxytaxol by human cytochrome P450 2C8. Cancer Res **54,** 5543, 1994.
51. Nahmias, Y., Schwartz, R.E., Verfaillie, C.M., and Odde, D.J. Laser-guided direct writing for three-dimensional tissue engineering. Biotechnol Bioeng **92,** 129, 2005.
52. Nahmias, Y., and Odde, D.J. Micropatterning of living cells by laser-guided direct writing: application to fabrication of hepatic-endothelial sinusoid-like structures. Nat Protoc **1,** 2288, 2006.

Address correspondence to:
Padmavathy Rajagopalan, Ph.D.
Department of Chemical Engineering
Virginia Polytechnic Institute and State University
133 Randolph Hall
Blacksburg, VA 24061

E-mail: padmar@vt.edu

Received: October 21, 2009
Accepted: April 6, 2010
Online Publication Date: May 17, 2010